LOW ORDER MODELLING AND PID-TYPE FUZZY LOGIC CONTROL USING MULTIPLE SENSORS

P. J. Escamilla-Ambrosio*, N. Mort†

*Department of Aerospace Engineering, University of Bristol, Queens Building, University Walk, Bristol BS8 1TR, UK
(Telephone: +44 (0) 117 928 9860, Fax: +44 (0) 117 927 2771, E-mail: J.Escamilla@bristol.ac.uk).
†Department of Automatic Control and Systems Engineering, University of Sheffield, Mappin Street, Sheffield S1 3JD, UK
(Telephone: +44 (0)114 222 5559, Fax: +44 (0)114 273 1729, E-mail: n.mort@sheffield.ac.uk).

Keywords: Low-order modelling, PID Control, Fuzzy control, Multi-sensor data fusion, Adaptive Kalman filter.

Abstract

In this work a novel approach to deal with the noise issue in both the auto-tuning procedure and the control performance for a PID-type fuzzy logic controller in a multi-sensor environment is proposed. This approach combines a low-order modelling method with a fuzzy logic-based adaptive decentralised Kalman filtering approach. The proposed methodology is tested in several simulated benchmark processes. Good results are obtained.

1 Introduction

In this paper a combination of three recently developed approaches: 1) the low-order modelling method proposed by Wang *et al* [7], 2) the modified hybrid PID-type fuzzy logic controller developed by Escamilla and Mort [4], and the fuzzy logic-based adaptive decentralised Kalman filter, also proposed by Escamilla and Mort [5], is proposed to deal with the noise issue in both the auto-tuning procedure and the control performance of a PID-type fuzzy logic controller in a multi-sensor environment. It is assumed that multiple sensors, which may have different accuracy levels (different measurement noise amplitudes), are used to determine the process output. The idea of using multiple sensors and fusion is to have a reliable control that can operate at good accuracy levels even in the occurrence of sensor failures.

Therefore, in the remaining of this paper, first in section 2 the general structure for system identification and control designing is explained. Then, the different functional blocks are described. After that, in section 3 several examples are presented to illustrate the effectiveness of the proposed approach. Finally, in section 4 conclusions to this work are given.

2 General system identification and control structure

The general system identification and control structure proposed in this work is shown in figure 1. This structure

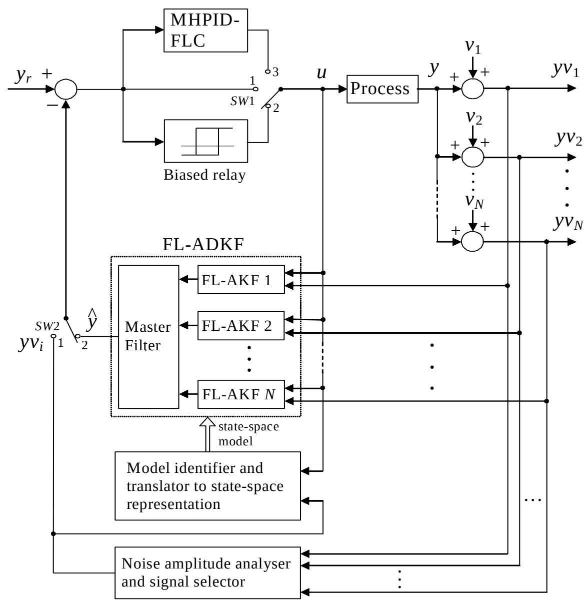

Figure 1: General system identification and control structure.

consists of several functional blocks. A biased relay feedback experiment is used to find the process critical point information and the steady-state gain. A noise amplitude analyser and signal selector is used to estimate the noise bands and the noise covariance in each sensor. Also, this block selects the signal with the least noise band to perform with it a biased relay experiment. The data obtained from this experiment is used by a model identifier to approximate the process transfer function as a first order plus dead-time. The obtained transfer function is transformed to its discrete state-space representation. This state-space model is used by N fuzzy logic-based adaptive Kalman filters (FL-AKFs) configured in a fuzzy logic-based adaptive decentralised Kalman filter (FL-ADKF). The FL-ADKF fuses and filters all the noisy measurements signals. The fused estimated process output $\hat{y}$ is used as measurement signal to compare with it the reference signal and calculate the error signal. The error signal is fed to a controller referred to as modified hybrid PID fuzzy logic controller (MHPID-FLC). In the next sections, each one of the functional blocks in figure 1 are briefly explained.

2.1 Model identifier and translator to state-space representation

A large number of processes can be characterised by the first-order plus dead-time model [6]:

$$G(s) = \frac{Ke^{-Ls}}{Ts+1} \quad (1).$$

For these kinds of processes Wang *et al* [7] have recently proposed a biased relay feedback test from which the critical point and the static gain can simultaneously be obtained. By applying the biased relay feedback, shown in figure 2(a), to a process of the kind (1), the obtained process input *u* and the process output *y* are shown in figure 2(b). For these processes the output *y* converges to the stationary oscillation in one period $(T_{u1}+T_{u2})$, and the oscillation is characterised by:

$$A_u = (\mu_0+\mu)K(1-e^{-L/T}) + \varepsilon\, e^{-L/T} \quad (2)$$

$$A_d = (\mu_0-\mu)K(1-e^{-L/T}) - \varepsilon\, e^{-L/T} \quad (3)$$

$$T_{u1} = T\ \ln\frac{2\mu Ke^{L/T}+\mu_0 K-\mu K+\varepsilon}{\mu K+\mu_0 K-\varepsilon} \quad (4)$$

$$T_{u2} = T\ \ln\frac{2\mu Ke^{L/T}-\mu K-\mu_0 K+\varepsilon}{\mu K-\mu_0 K-\varepsilon} \quad (5).$$

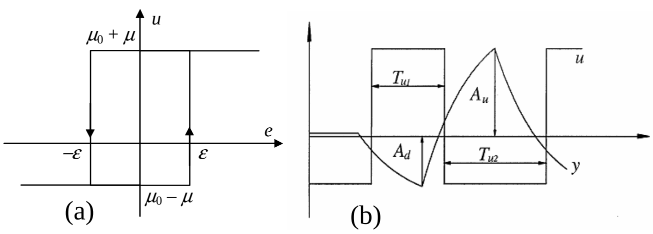

Figure 2: (a) biased relay, (b) waveforms under a biased relay feedback.

The above four equations are the accurate expressions for the period and the amplitude of the limit cycle oscillation of the first order plus dead-time process. Therefore, by measuring any three of A_u, A_d, T_{u1}, and T_{u2}, the parameters of the model *K*, *T* and *L* can be calculated from (2) to (5). Solving these equations is a tedious task. However, the calculations can be simplified if *K* is obtained by an alternative procedure. This procedure consists in calculating *K* as the ratio of DC components in the output and input:

$$K = \frac{\int_0^{T_{u1}+T_{u2}} y(t)\,dt}{\int_0^{T_{u1}+T_{u2}} u(t)\,dt} \quad (6).$$

Having available the value of *K*, the normalised dead-time of the process Θ=L/T can be obtained from (2) as:

$$\Theta = \ln\frac{(\mu_0+\mu)K-\varepsilon}{(\mu_0+\mu)K-A_u} \quad (7).$$

It then follows from (4) that:

$$T = T_{u1}\left(\ln\frac{2\mu Ke^{\Theta}+\mu_0 K-\mu K+\varepsilon}{\mu K+\mu_0 K-\varepsilon}\right)^{-1} \quad (8).$$

Finally, the dead time is calculated as:

$$L = T\Theta \quad (9).$$

If the process to be identified is of the form (1) and there is no measurement noise, then the parameters obtained with the biased relay method gives an almost exact identification of the process parameters. Furthermore, because in practice many high-order processes can be well approximated by first-order plus dead-time models, the biased relay method can also be used to model processes of higher order [7]. Therefore, this low-order modelling is accurate enough for PID control design in most cases.

The above method still gives good results for the case where there is noise in the measurements. However, in that case, the parameters *K*, A_u, and A_d have to be calculated by averaging over those values obtained over several cycles. It is recommended to average over eight cycles of stationary oscillations [7].

Therefore, once the biased relay experiment is carried out, an approximated model of the process is available as a first-order transfer function. In order to use this model in the FL-AKFs (see figure 1) it is necessary to translate it to its state-space representation. This is performed in two stages. First, the transfer function in continuous time is transformed to its corresponding state-space representation. Second, having available the continuous state-space representation, this is translated to its corresponding discrete form. Thus, having available the process model in its discrete state-space representation, this model can be used by the FL-ADKF to perform multi-sensor data fusion (MSDF).

2.2 Noise amplitude analyser and signal selector

The noise amplitude analyser and signal selector performs several tasks. First, it determines the noise bands in each sensor. The noise band can be estimated by measuring the peak-to-peak amplitude of the output signal when the process is in steady-state [1]. Second, an estimation of the measurement noise covariance value, R_i, of each sensor is performed over the data collected during a certain period of time. Finally, the signal with the minimum noise band is selected as the output signal of this block.

2.3 Fuzzy logic-based adaptive decentralised Kalman filter

In the standard decentralised Kalman filter (SDKF) algorithm the information is processed in two stages. In the firs stage, *N* local standard Kalman filters (SKFs) process their own data in parallel to yield the best possible local estimates. In the second stage, a master filter fuses the local estimates, yielding the best global estimate [2]. The structure of the FL-ADKF is similar to that of the SDKF, but instead of having N local SKFs there are considered N local FL-AKFs working in parallel [5]. The adaptation in each FL-AKF is in the sense of dynamically tuning the measurement noise covariance matrix R or the process noise covariance matrix Q employing a fuzzy inference system (FIS) based on a covariance matching technique. For a matter of space the complete description of the FL-AKF cannot be presented here. The reader interested is referred to [3, 5].

2.4 The modified hybrid PID-type fuzzy logic controller

The structure of the modified hybrid PID-type fuzzy logic controller (from here referred to as MHPID-FLC) is presented in figure 3(a). The fuzzy control system (FCS) inside the MHPID-FLC structure consists of four fuzzy rules:

R_1: If E is N and CE is N then $u = p_1*E + q_1*CE + r_1$
R_2: If E is N and CE is P then $u = p_2*E + q_2*CE + r_2$
R_3: If E is P and CE is N then $u = p_3*E + q_3*CE + r_3$
R_4: If E is P and CE is P then $u = p_4*E + q_4*CE + r_4$

where the coefficient constants $p_i = q_i = 1$, and $r_i = 0$; for i = 1, 2, 3, 4. The linguistic labels for the fuzzy sets mean P = Positive and N = Negative, they are shown in figure 3(b).

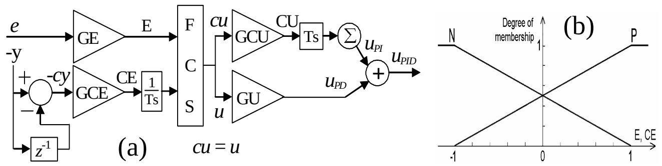

Figure 3: (a) MHPID-FLC structure, (b) Fuzzy sets.

Based on	GE	GCE	GU	GCU
K_u, T_u	1	$\frac{1}{4}*T_u$	$0.3*K_u$	$1.2*\frac{K_u}{T_u}$
K_P, K_I, K_D	1	$2*\frac{K_D}{K_P}$	$\frac{K_P}{2}$	K_I
K_P, T_i, T_d	1	$2*T_d$	$\frac{K_P}{2}$	$\frac{K_P}{T_i}$

Table 1: Relationship between the scaling factors of the MHPID-FLC, the traditional PID control gains, and the Ziegler Nichols frequency response tuning formulae.

The control output of the MHPID-FLC is equivalent to its traditional counterpart with $\beta = 0.5$ [4]:

$$u_{PID_k} = K_P * \beta * y_{r_k} - K_P y_k + K_I * \sum_{i=0}^{k} e_i * Ts - K_D * \frac{cy_k}{Ts} \qquad (10).$$

The scaling factors of the MHPID-FLC can be calculated from the traditional PID gains or from the ultimate gain and the ultimate frequency obtained from a relay experiment [4]. Table 1 gives the formulae for these calculations.

2.5 Identification and auto-tuning procedure using multiple noisy sensors

Therefore, from the previous sections and referring to figure 1, the proposed identification and auto-tuning procedure is summarised as follows:

1. *SW1* is in position 1; *SW2* is in position 1. First, in the "listening period", 0-12 sec, the noise bands and the measurement noise covariance in each sensor are estimated. The sensor signal with the smallest noise band is selected to be feedback to the biased relay.
2. *SW1* switches to position 2 and a biased relay is applied at time t = 12 sec.
3. Data is registered over five cycles of stationary oscillations. By averaging the values obtained over these five cycles, the parameters K, A_u, and A_d are calculated and the values of T_{u1} and T_{u2} are measured over the fifth cycle. With these parameters, the value of the normalised process Θ is calculated using (7). Similarly, T is calculated from (8). Then, the dead time L is calculated from (9) and the process transfer function is modelled as a first-order plus dead-time. The obtained transfer function is transformed to its corresponding continuous and discrete state-space representations.
4. At the end of the fifth cycle all the FL-AKFs are activated using the state-space representation of the plant and MSDF is performed using the FL-ADKF; then the fused output is used as process output, *SW2* is switched to position 2. The initial conditions for the FL-AKFs are defined as $x_i(0) = 0$, $\hat{x}_i(0) = 0$, $i = 1,2,\ldots,N$. Because an estimation of the measurement noise covariance value R_i for each sensor has been obtained in step 1, these values are used in the corresponding FL-AKFs. Therefore, while the covariance values R_i are assumed to be known, they are not adapted in the FL-AKFs. Instead, the unknown values of the process noise covariance matrices Q_i, which represent the uncertainty in the process model, are the ones that are adaptively adjusted in the FL-AKFs. This will compensate for the modelling errors, recalling that the model used is an approximated model.
5. During the sixth cycle, the ultimate gain and the ultimate frequency are calculated as:

$$K_u = \frac{4\mu}{\pi(A_u + |A_d|)/2} \qquad (11)$$

$$T_u = T_{u1} + T_{u2} \qquad (12)$$

where μ is the value of the relay amplitude when the bias is taken out.

6. With K_u and T_u available, the scaling factors of the MHPID-FLC are calculated using the formulae given in Table 1.
7. Finally, at the end of oscillation 6, *SW1* is switched to position 3 and the loop MHPID-FLC – process is closed.

Afterwards, the performance of the controller can be investigated by introducing a set-point change and a load-disturbance at particular time steps. In order to test the effectiveness of the proposed approach, three examples are presented in the next section.

3 Illustrative examples

The viability of the previously described approach is demonstrated by simulating three processes taken from [7]. The experiments were developed under the Matlab/Simulink simulation environment. It is assumed that there are two sensors in the scheme shown in figure 1. The measurement noise in each sensor, for all the experiments, is defined as a Gaussian zero-mean white noise sequence with variances 0.008 and 0.033 for v_1 and v_2, respectively.

The FCS inside the MHPID-FLC works with normalised inputs, in the range [-1, 1]. This normalisation is carried out by dividing the inputs between the maximum range of variation of the error signal, which in this case is assumed to be [-10, 10]. Therefore, the normalisation factor is (1/10) applied to both inputs, e and $-y$. Obviously, the controller output needs to be denormalised; hence, the controller output is multiplied by a denormalisation factor, 10 in this case.

The processes studied and the corresponding parameters obtained from the biased relay experiment are listed in Table 2. The scaling factors of the MHPID-FLC obtained from the auto-tuning procedure for each process are shown in Table 3. In order to analyse the set-point and load-disturbance responses, a step change of 10 units and a load disturbance, also of 10 units, are applied at appropriate time steps. The set-point and load-disturbance responses under MHPID-FLC for the plant in examples 1, 2 and 3 are shown in figures 4(a), 5(a), and 6(a), respectively. From these figures it can be noted that slightly sluggish set-point and load-disturbance responses are obtained. This is more noticeable in examples 2 and 3. However, the control performance can be further improved by modifying the value of the consequent parameters, p, q and r, in the fuzzy rules of the FCS inside the MHPID-FLC structure. Therefore, to improve the control performance, the consequent parameters are modified as is indicated in table 4. The improved set-point and load-disturbance responses under MHPID-FLC for the plants in examples 1, 2 and 3 are shown in figures 4(b), 5(b), and 6(b), respectively. Note that the scaling factors found in the auto-tuning procedure are left unchanged.

Note in figures 4 to 6 that as the order of the process increases, less noise is filtered by the FL-ADKF. In other words, this means that a quite accurate model is obtained when the plant is effectively of first-order. However, if the order of the plant increases, then the accuracy of the approximated model decreases. As a result, the value of the process noise covariance Q, which is adaptively adjusted, is increased to take into account this increased modelling error. This can be appreciated in figure 7, where the values of R_1(t) and Q_1(t) in the FL-AKF 1, fed by sensor 1, are plotted for each one of the examples. Remember that R and Q control the bandwidth of the filter. Thus, while R is maintained constant, Q is constantly changing increasing or decreasing the bandwidth of the filter and, in consequence, increasing or reducing the filtering action.

Example	Process	Biased relay test results				Model parameters		
		T_{u1}	T_{u2}	A_u	A_d	K	T	L
1	$\frac{e^{-2s}}{2s+1}$	3.35	4.0	1.714	-1.302	1.009	1.871	2.021
2	$\frac{e^{-2s}}{(2s+1)^2}$	5.55	6.45	1.543	-1.267	1.18	4.585	2.849
3	$\frac{e^{-0.5s}}{(s+1)(s^2+s+1)}$	2.95	3.35	2.106	-1.672	1.215	1.592	1.892

Table 2: Estimated parameters from biased relay experiment.

Example	Process	Scaling factors MHPID-FLC			
		GE	GCE	GCU	GU
1	$\frac{e^{-2s}}{2s+1}$	1	1.837	0.2757	0.5065
2	$\frac{e^{-2s}}{(2s+1)^2}$	1	3.0	0.1812	0.5437
3	$\frac{e^{-0.5s}}{(s+1)(s^2+s+1)}$	1	1.575	0.2568	0.4045

Table 3: Scaling factors obtained from the auto-tuning procedure.

Example	Process	Consequent parameters				Modified cons. parameters			
		Rule	p	q	r	Rule	p	q	r
1	$\frac{e^{-2s}}{2s+1}$	1	1	1	0	1	1.8	0.3	0
		2	1	1	0	2	0.4	0.4	0
		3	1	1	0	3	0.4	0.4	0
		4	1	1	0	4	1.8	0.3	0
2	$\frac{e^{-2s}}{(2s+1)^2}$	1	1	1	0	1	2.3	0.5	0
		2	1	1	0	2	0.4	0.4	0
		3	1	1	0	3	0.4	0.4	0
		4	1	1	0	4	2.3	0.5	0
3	$\frac{e^{-0.5s}}{(s+1)(s^2+s+1)}$	1	1	1	0	1	2.5	0.2	0
		2	1	1	0	2	0.1	0.1	0
		3	1	1	0	3	0.1	0.1	0
		4	1	1	0	4	2.5	0.2	0

Table 4: Modified consequent parameters.

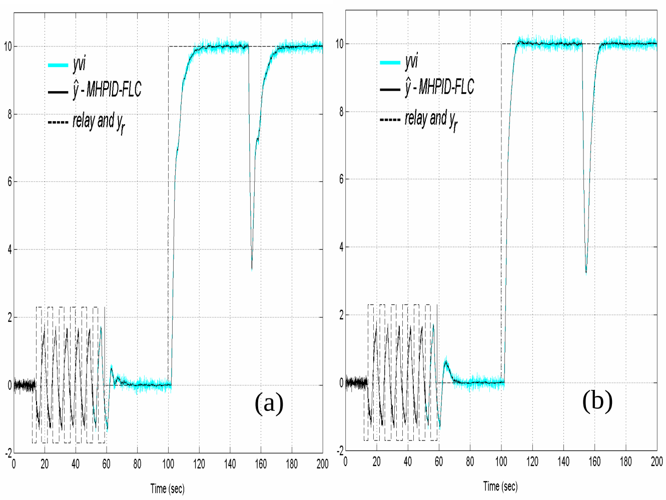

Figure 4: Set-point and load-disturbance responses for the plant in example 1, (a) with original consequent parameters, (b) with modified consequent parameters.

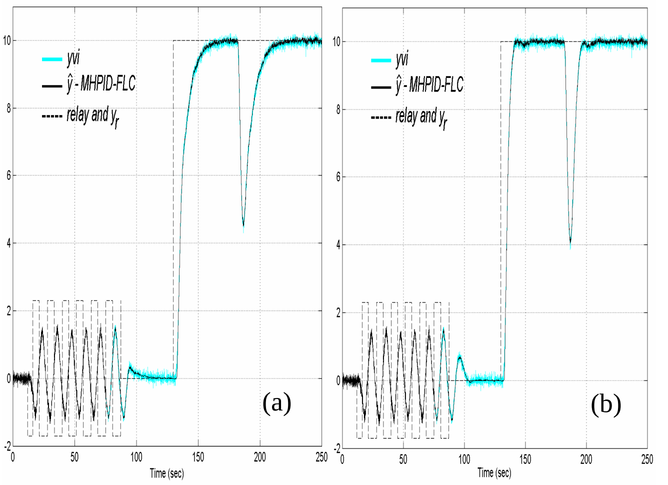

Figure 5: Set-point and load-disturbance responses for the plant in example 2, (a) with original consequent parameters, (b) with modified consequent parameters.

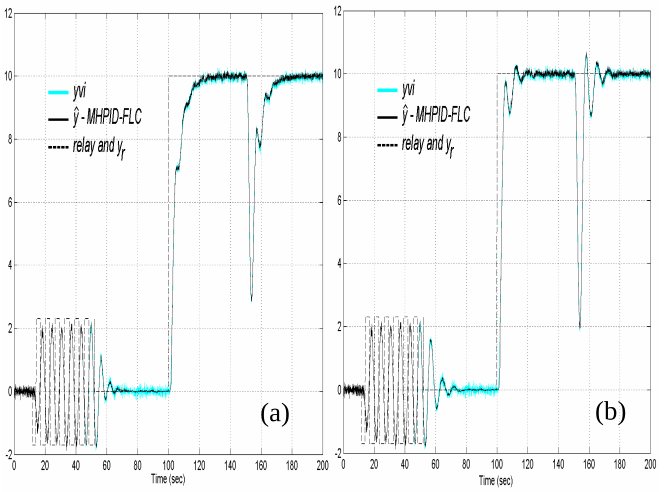

Figure 6: Set-point and load-disturbance responses for the plant in example 3, (a) with original consequent parameters, (b) with modified consequent parameters.

Therefore, from the results obtained in the simulated examples, it was demonstrated that the described auto-tuning procedure is effective when there are multiple noisy sensors measuring the process output. Good results of MSDF and signal filtering also were obtained.

4 Conclusions

In this paper a novel approach to deal with the noise issue in both the auto-tuning procedure and the control performance for a MHPID-FLC, in a multi-sensor environment has been proposed. This approach combines a low-order modelling method with the FL-ADKF approach. The proposed methodology was tested in several simulated benchmark processes. Good results were obtained.

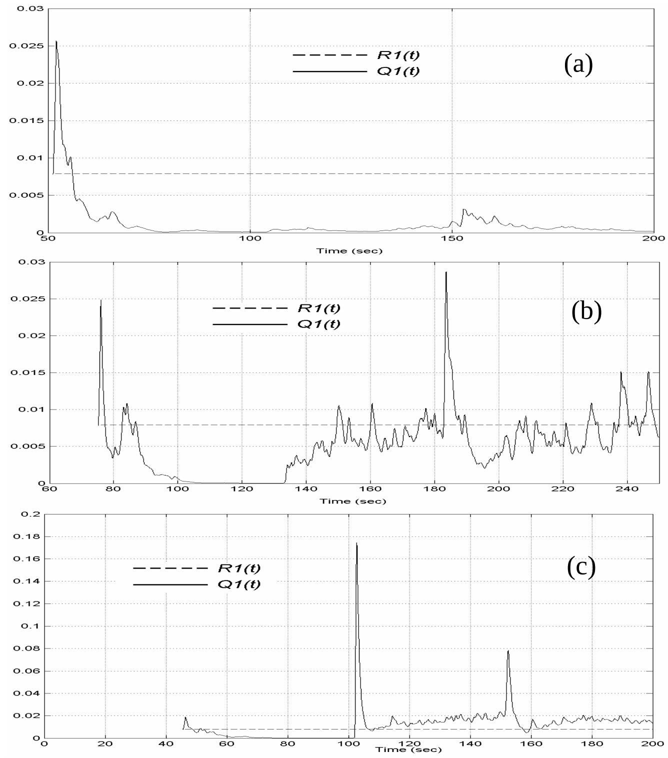

Figure 7: (a) Values of $R_1(t)$ and $Q_1(t)$ in the FL-AKF 1, fed by sensor 1, example 1; (b) Values of $R_1(t)$ and $Q_1(t)$ in the FL-AKF 1, fed by sensor 1, example 2; (c) Values of $R_1(t)$ and $Q_1(t)$ in the FL-AKF 1, fed by sensor 1, example 3.

References

[1] K. J. Astrom, T. Hagglund, C. C. Hang and W. K. Ho. "Automatic tuning and adaptation for PID controllers – A survey", *Control Eng. Practice*, **1**, pp. 699-714, (1993).

[2] R. G. Brown and P. Y. C. Hwang. *Introduction to random signals and applied Kalman filtering whit MATLAB exercises and solutions*, Third edition, John Wiley & Sons, New York, (1997).

[3] P. J. Escamilla-Ambrosio and N. Mort. "Development of a fuzzy logic-based adaptive Kalman filter", *Proceedings of the European Control Conference ECC'01*, September 4-7, Porto, Portugal, pp. 1768-1773, (2001).

[4] P. J. Escamilla-Ambrosio and N. Mort. "Auto-tuning of fuzzy PID controllers", *In CD ROM Proceedings of the XV IFAC World Congress*, July 21-26, Barcelona, Spain, (2002).

[5] P. J. Escamilla-Ambrosio and N. Mort. "Hybrid Kalman filter-fuzzy logic adaptive multisensor data fusion architectures", Proceedings of the 42nd IEEE Conference on Decision and Control, Maui, Hawai, USA, December 9-12, pp. 5215-5220, (2003).

[6] D. E. Seborg, T. F. Edgar and D. A. Mellichamp. *Process dynamics and control*, Wiley, New York, (1989).

[7] Q. –G. Wang, C. –C. Hang and B. Zou. "Low-order modeling from relay feedback", *Ind. Eng. Chem. Res.*, **36**, pp. 375-381, (1997).